Lewis salts may be important as intermediates or transition states in catalytic reactions. An example in this category is the catalysis of CO exchange with $Fe(CO)_4P(C_5H_5)_3$ via an acidic medium.[68]

(68) F. Basolo, A. T. Brault, and A. J. Poë, J. Chem. Soc., 676 (1964).

The "Solid-State" Properties of Rigid Organic Solutions

ANDREAS C. ALBRECHT

Department of Chemistry, Cornell University, Ithaca, New York

Long ago it was found that a variety of crystalline, inorganic solids were capable of slowly releasing stored energy in the form of visible light after irradiation in the visible or ultraviolet region or at the much higher energies of X-rays and γ-rays. These solids came to be known as crystal phosphors or simply "phosphors."[1] Not only do such sensitized solids exhibit afterglow, but they can also be photoconductive. Furthermore, the release of the stored energy can be variously hastened or retarded by the application of stimuli such as heat, infrared light, or electric fields. The modern theory of ordered solids, including impurity centers or defects, manages to embrace this class of crystalline materials quite successfully. What is quite remarkable is that over the past decade or so there has emerged a class of amorphous, organic solids having properties almost identical with those of the inorganic crystal phosphors.

These organic solids normally consist of simple dilute organic solutions which are converted to a rigid but noncrystalline state by cooling. Alternatively, polymerization into a rigid state is possible. Sensitization can be accomplished, as before, by high-energy irradiation or by photoexcitation. In the former case it is principally the solvent molecule which captures the energy, simply because it constitutes the bulk of the material. Photoexcitation is much more selective and occurs via the solute molecule whose spectrum normally appears at wavelengths to the red of the solvent absorption. In either case it seems that a large amount of the energy is stored through ionization or the separation of charges within the solids (an internal photoelectric effect).

The recombination of charges can lead to excited electronic states which may decay by radiative means giving rise to the "afterglow" of organic phosphors. Usually the afterglow is a luminescence characteristic of the solute molecule. Even in the case where the solvent is the primary absorber, solute emission can be seen because positive "holes" in the solvent are often mobile. When these are captured by the neutral solute molecule, the sensitized solid becomes similar to that in which the solute molecule is directly photoionized.

As we have indicated, these sensitized organic solids exhibit the full array of phosphor-like properties. These include photoconductivity, thermoluminescence (recombination luminescence seen upon heating), photostimulated emission (enhanced recombination luminescence through infrared or visible illumination), and electric stimulation (perturbation of the recombination luminescence by an externally applied electric field). The afterglow itself, seen at a given, fixed temperature, is conveniently called isothermoluminescence (ITL).

A nomenclature for these phosphor-like properties has developed which attempts to distinguish the two types of primary energy storage steps. Thus, when the activation step is by high-energy irradiation, the term "radio" appears somewhere in the name, whereas with visible or ultraviolet illumination, "photo" is used. Unfortunately, consistent rules have not been applied. Thus "radiophotoluminescence" is a luminescence released by photostimulation of a solid which has been previously sensitized by high-energy radiation. On the other hand electrophotoluminescence is the luminescence seen when an electric field is applied to a solid previously sensitized by ultraviolet illumination. Were the solid sensitized by high-energy irradiation one could use the term electroradioluminescence.

A number of laboratories have been active in studying the phosphor-like properties of irradiated organic solids (including polymers) during the past decade. In our own laboratory, we have been preoccupied with what we feel is a prototype rigid organic solution. The system consists of a solution of $\sim 10^{-3}$ M N,N,N',N',-tetramethyl-p-phenylenediamine (TMPD) in the solvent 3-methylpentane (3-MP) at 77°K. Our interest in this system arose from the early work on polarized photoionization (photodichroism) of rigid organic solutions carried out in the laboratories of Lewis at Berkeley in the 1940's.

(1) For a survey of the field of inorganic, crystalline phosphors a useful reference is P. Pringsheim, "Fluorescence and Phosphorescence," Interscience Publishers, New York, N. Y., 1949, Chapter VII.

In this earlier work, the rigid nature of the solution was important to fix the photochemistry as well as the orientation of the photoproduct. We now see that the rigidity is what confers upon these materials their "solid state" or phosphor-like properties. From our own work there has emerged a unified and simple picture of this solid which appears to account for most of its properties. The model relies heavily on the presence of preexisting electron-trapping cavities in the solid; it relies on the thermal, electric, and photomobilizability of the trapped electrons: and it strongly emphasizes the role played by the long-range Coulomb potential of the solute cation in governing the diffusion of the mobilized electron.

We wish to emphasize that this Account is by no means a review of the field. Readers desiring a comprehensive review are directed to that of Willard.[2] It therefore takes the liberty of a bias heavily centered upon our own experience. Thus attention is confined almost uniquely to the TMPD–3-MP prototype solid in which the primary energy storage step is by photoionization. We feel that the results and the model proposed to explain them are of general validity, although we will not attempt to document this.

The material to be discussed naturally falls into two categories. The first involves the energy storage step itself—the photoionization of the solute molecule. This step turns out to be a biphotonic one of considerable subtlety. It generates mobile electrons, later trapped, and stationary cations. If the mobile electrons are polarized in an externally applied electric field, a photocurrent is seen. The cation is the radical ion resulting from removal of an electron from TMPD; it has a distinctive molecular spectrum in the visible region and has long been known as Wurster's Blue (WB). Kinetic studies of the rise of photocurrent and of the appearance of the cation spectrum both reveal the biphotonic requirements for ionization but have appeared to call for different intermediate states, a puzzle which only very recently has been clarified. The question of whether the primary energy storage is "unimolecular" in the sense that the majority of charge pairs created by photoionization remains correlated once the mobilized electron becomes trapped in the matrix has been resolved through recombination luminescence studies.

The second category of material to be presented deals with the properties of the photosensitized solid itself. These include the recombination luminescence as seen under various stimuli and the secondary photoconductivity signals which arise by the photoionization of trapped electrons. The electric stimulation of the recombination luminescence provides an especially lucid view of the sensitized organic solid. At the same time it raises a most unusual and unanswered question regarding the average electron distribution about the cationic Coulomb center.

An abbreviated and descriptive version of the model will be presented and a brief discussion will show how it manages to explain the general "solid state" properties of these organic solids.

The Energy-Storage Step

A. The Photoionization. When a 10^{-3} M solution of TMPD in 3-MP is cooled to 77°K it becomes a solid having a viscosity of $\sim 10^{12}$ P[3]—nearly that of ordinary window glass. This solution is transparent in the near-infrared and visible region and absorbs only in the near-ultraviolet at the onset of TMPD absorption at about 350 nm. This solid is an extremely good insulator exhibiting a resistivity of $> 10^{19}$ ohm cm. In thin samples it can withstand applied electric fields in excess of 10^6 V/cm. The solution appears to be a genuinely amorphous body which does not depolarize light to any significant extent.

When this solid is illuminated with near-infrared ($\lambda < 1.6$ μ), visible, or very-near-ultraviolet light ($\lambda > 350$ nm) it undergoes no detectable changes whatever. However, when the onset of TMPD absorption is reached in the ultraviolet ($\lambda < 350$ nm), the incident light is absorbed and a purple coloration develops which is due to the spectrum of Wurster's Blue (see Figure 1). With greater effort it is also possible to see a very broad absorption band occupying the near-infrared region and peaking around 1.5 μ. This turns out to be the spectrum of the matrix-trapped electron. Furthermore, if the sample is in a photoconductivity cell, buildup of a photocurrent can be seen. Since it is known[3] that the WB cation is unable to rotate—much less translate—in these solids, the electron must be the charge carrier responsible for the photocurrent. Thus the appearance of new spectra and the photoconductive properties, each in its own distinct fashion, indicate the storage of light energy by photoinduced charge creation and separation. These events are now briefly examined in more detail.

1. The Growth of the Cation Spectrum. The kinetics of the growth of the cation spectrum has been studied in great detail in our laboratory by Cadogan.[4] In brief, it has been shown that at least two photons are required to generate one cation and that the mechanism is one which involves the triplet state of TMPD as an intermediate state. The first photon must be $\lambda < 350$ nm to produce TPMD triplet (*via* excited singlet). The second photon ionizes the triplet with the onset of threshold at about 400 nm. The ionization of an oriented triplet state is found to be isotropic with respect to polarization of the second photon beam. This is interpreted as indicating ionization into a continuum or near-continuum of levels at or near the true ionization (full charge separation) threshold of TMPD in this system (~ 5.9 eV here *vs.* ~ 6.7 eV in gas).

2. Photoconductivity Studies. The first observation of photoconductivity in such rigid organic solutions was

(2) J. E. Willard in "Fundamental Processes in Radiation Chemistry," P. J. Ausloos, Ed., Interscience, New York, N. Y., 1969, Chapter 9.

(3) J. R. Lombardi, J. W. Raymonda, and A. C. Albrecht, *J. Chem. Phys.*, **40**, 1148 (1964).

(4) K. D. Cadogan and A. C. Albrecht, *J. Phys. Chem.*, **72**, 929 (1968).
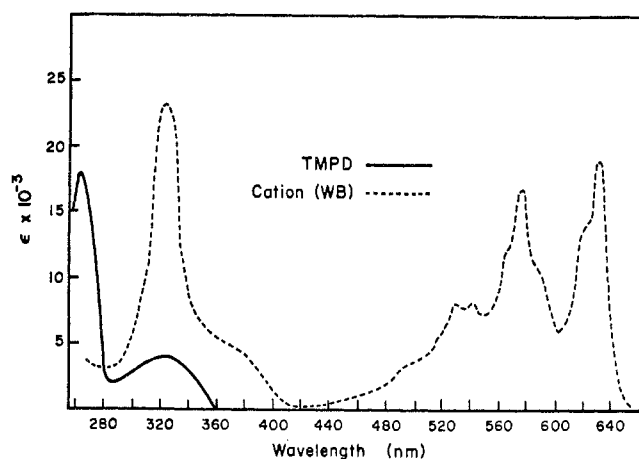
Figure 1. The absorption spectra of TMPD (solid curve) and its one-electron oxidation product WB (dotted curve) in 3-MP at 77°K. The actual conversion of TMPD to WB rarely exceeds ~1%. The WB spectrum, when diminished by a factor of 100, is seen not to represent a drastic change in the spectral properties of the solid. (The trapped-electron spectrum, which peaks in the near-infrared and extends through the visible and into the ultraviolet, is not shown here.)

made more than a decade ago,[5] and this work has been greatly amplified since then.[6,7] Of crucial importance for the discovery of such signals was the use of very thin samples (~1 mil) in order that very high electric fields could be imposed. A typical sample, $10^{-3} M$, is contained as a 10^{-3}-in. sandwich between semitransparent electrodes at 77°K. Monochromatic illumination (~5 nm band width) is employed normal to the front electrode and a primary–secondary double-beam technique is used when necessary (one beam for each photon). Various photoelectric effects are displayed in Figure 2. The typical photoconductivity signals seen in a single-beam study are shown in Figures 2a,b. The sample is initially completely insensitive to near-infrared, visible, or even near-ultraviolet light (the secondary region, $\lambda > 350$ nm) as before. Only after the region of primary TMPD absorption is entered ($\lambda < 350$ nm) does a photocurrent develop. The level is about 10^{-11} A over a dark current of about 3×10^{-14} A. Following sensitization, two new types of photoconductive behavior are evident. First, a photocurrent spike can be excited anywhere in the previously insensitive infrared, visible, and near-ultraviolet region ($\lambda > 350$ nm). Second, in the very-near-ultraviolet (the 365-nm Hg line is convenient here), the spike appears superimposed upon a new, quasi-steady-state, signal which corresponds to a second type of induced or sensitized photoelectric property of the solid (Figure 2b). These induced photoelectric signals will be discussed more completely later for they are genuine phosphorlike properties of the solid.

When the electrodes are electrically blocked using thin quartz spacers, the primary photocurrent signal exhibits the pattern of a polarization current as shown

in Figure 2c. This observation demonstrates the bulk nature of the conductivity and indirectly indicates that electrons flowing across macroscopic distances in the solid are responsible for the conductivity. When the electrodes are blocked, an internal field evidently builds up as the mobile electrons accumulate at the electrode. This field then serves to drive a negative photocurrent (Figure 2c) once the applied field is removed. The absence of polarization type signals in the primary region when the electrodes are not blocked (Figure 2a,b) indicates that the primary signal is not due to a photodielectric effect. For example, one could imagine that the photoproduction of dipolar centers (partial ionizations) could lead to a steady charging of the electrodes. However, the quality of such signals should not change when the electrodes are blocked.

The analysis of primary photocurrent rises on a short time scale has led to the discovery of the biphotonic nature of the ionization.[6,7] There may actually occur two different intermediates which are one photon ionized depending on the conditions of illumination. Intense, broad-band excitation appears to favor a nontriplet intermediate[6,7] (a solute–rigid solvent charge-transfer state is a likely candidate). By contrast, single-beam, monochromatic irradiation clearly demonstrates the triplet intermediate.[7]

An excellent display both of the biphotonic nature of the ionization and the triplet-state intermediate in photoconductivity is seen in Figure 2d. Here, with primary excitation only, the incident light is abruptly halved in intensity. First the photocurrent abruptly drops to one-half its previous level (one-photon ionization of the intermediate) and then the signal slowly decays further (with the triplet lifetime) by another factor of two as the intermediate state passes to its new level—one-half that of its previous value.

B. The Fixing of the Charge Separation (Storage). Photoconductivity is attributable to a very small number of mobile electrons and is seen in both rigid and soft solutions. Energy storage, on the other hand, comes about only when the charge-separated condition is frozen into the solid. Both the cation and the electron must be trapped. While the rotational relaxation studies[3] prove that the cation is trapped by the high viscosity, the nature of the trapping of the electron is not immediately obvious. To localize an electron in a solid it is only necessary that the immediate surroundings of a given volume element present an energy barrier for thermal escape to the electron *and* that this volume element be sufficiently large not to require inordinate kinetic energy of localization (uncertainty principle). Electron affinity of the usual sort is not a requirement. In fact, we strongly favor the view[6] that the energy barrier itself arises from uncertainty principle considerations. The 3-MP solid possesses frozen-in, preexisting density fluctuations; in their extreme form the rarefactions are "cavities."[8] An electron in a sufficiently large cavity may be delocalized in three di-

(5) A. C. Albrecht and M. E. Green, J. Chem. Phys., 31, 261 (1959).
(6) G. E. Johnson and A. C. Albrecht, ibid., 44, 3162, 3179 (1966).
(7) K. D. Cadogan and A. C. Albrecht, ibid., 51, 2710 (1969).

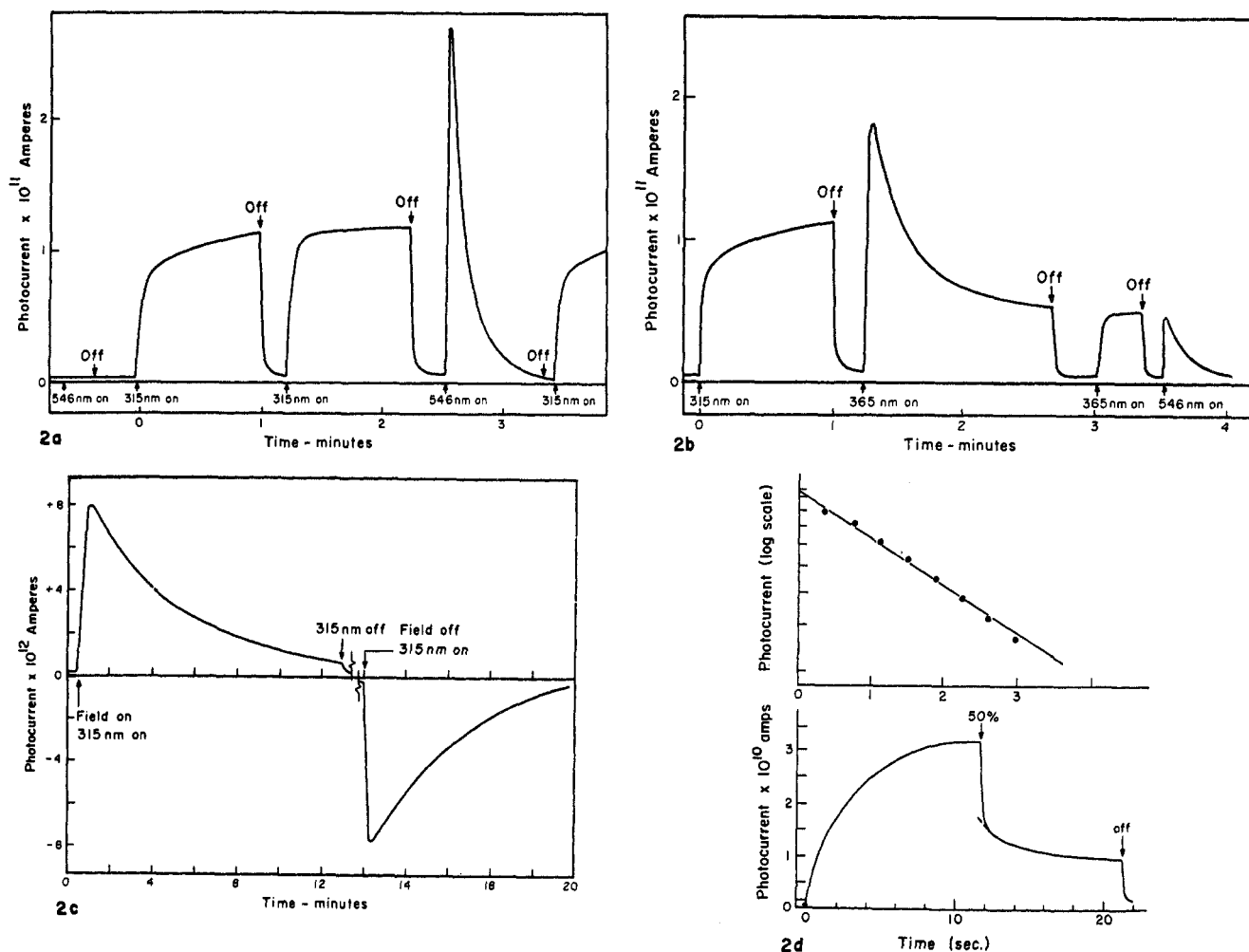(8) B. Wunderlich, J. Phys. Chem., 64, 1052 (1960).

Figure 2. Photoelectric signals in the TMPD–3MP solid. (a) Typical photocurrents seen in a 1-mil- (0.001 in.) thick TMPD–3MP ($\sim$2 $\times$ 10^{-3} M) solid at 77°K. The applied electric field is $\sim$2 $\times$ 10^{-5} V/cm. The absence of sensitivity in the visible region prior to ultraviolet (315 nm) sensitization is seen. The induced visible (546 nm) spike seen following sensitization is illustrated. (See ref 6.) (b) Photocurrent signals in the same system as in Figure 2a. Here the induced, quasistationary, "365" signal is seen. Prior to sensitization (315 nm) the sample is not sensitive to 365-nm light. The spike signal is also seen, first, superimposed upon the "365" signal and then what remains of it at 546 nm following a brief period of 365-nm excitation. (See ref 6.) (c) Typical photoelectric effects in a TMPD–3MP solid at 77°K when the electrodes are blocked with quartz plates. The sample is a 1-mil-thick sandwich between two 6-mil-thick quartz plates. The applied electric field is $\sim$4 $\times$ 10^4 V/cm. The negative photocurrent seen in the absence of an applied field demonstrates the freezing-in of a charge polarization in the first, field-on step. (See ref 6.) (d) The photocurrent rise in the TMPD–3MP system on the time scale of seconds. At 12 sec the incident light (at 313 nm) is reduced by 50%. The signal immediately falls to one-half its previous level. Then it is seen to decay to a final level one-fourth the original value (note nonzero dark current). The log plot of this decay is shown. It gives a decay time of 2.48 sec. The rise time is 2.40 sec. Both values compare well with the triplet lifetime of TMPD. (See ref 7 involving different apparatus than that of ref 6.)

mensions to permit a zero-point energy several kT (thermal energy) below that required if the electron were to "squeeze" into the immediate environment of higher density solvent surrounding the cavity. A sharp localization in one or two dimensions can easily raise the zero-point energy of an electron several kT (at 77°K) above that of an electron in a cavity with slight delocalization in three dimensions. The trapped electron may be mobilized by structural relaxations of the solvent, which in effect allow the cavity to diffuse, or the electron may be stimulated to escape over the surrounding barrier. It is believed that for all the *non-thermal* means for mobilizing the electron, at least, the latter mechanism is dominant.

This trapping model is distinguished from the electron "digging its own cavity" model in polar fluids (in liquid ammonia, for example) in that in the solid the holes are preexisting and the polarization of the environment is only electronic.[9] The concentration of cavities having sufficient size for trapping must be greater than 10^{-2} M judging by the concentration at which electron scavengers such as O$_2$ become competitive.

One particularly detailed view of the trapped electron comes from its recently discovered esr signal seen in 3-MP at 77°K. This signal is narrow and easily saturated, indicating a relatively weak coupling of the electron with its surroundings.[10] The esr signal fades in the dark at 77°K in the exact manner that our

(9) A very useful recent review which discusses excess electron states in liquids is that of S. A. Rice, *Accounts Chem Res.*, 1, 81 (1968).

(10) J. Lin, K. Tsuji, and F. Williams, *J. Chem. Phys.*, 46, 4982 (1967). See references in this note for other esr work on trapped electrons in organic solids.

infrared sensitivity (photocurrent spikes, etc.) disappears, showing a half-life of many minutes. The signal is also bleached by infrared light. Furthermore, matrix trapping disappears as an effective phenomenon as the sample is softened (by admixing isopentane[3]) or heated.[6,7] Energy storage in soft solutions even at 77°K becomes very inefficient. No infrared sensitivity is seen. Probably in the softer media, structural relaxations[8] mobilize the cavities leading to electron–cation recombination. Primary photoconductivity, which only requires mobile electrons, is unaffected. The addition of scavengers (as varied as O_2, CO_2, and benzene) at competitive concentrations ($\sim 10^{-2} M$) also succeeds in removing the infrared sensitivity, for now the trapped electron is more stabilized as O_2^-, CO_2^-,[11,12] or the benzene anion.[12] With scavengers, energy storage can be more efficient, but the usual phosphor properties of the solid are quenched since the energy release is now too slow. It seems that the matrix trapping in scavenger-free samples (in 3-MP at 77°K) provides just the proper balance between the magnitude of energy storage and the rate of energy release to permit the solid to exhibit its variety of phosphor-like properties. These are now described.

The Phosphor-Like Properties of the Photosensitized Solid

The most conspicuous properties of a TMPD–3MP solid which has been exposed to primary excitation at 77°K are its blue coloration due to the cation and its luminescence behavior. During the primary excitation the sample is seen to emit a blue-green light which is the usual ultraviolet-excited fluorescence and phosphorescence of TMPD. When the excitation is removed, the emission abruptly becomes green as the fluorescence immediately decays (in 7.3 nsecs),[13] leaving a slowly disappearing phosphorescence with a lifetime of 2.4 ± 0.1 sec. After ∼1 min of dark decay, a weak, greenish residual luminescence (or "afterglow") remains which represents the radiative release of stored energy through charge recombination. The manner of response of this luminescence to various perturbations, as well as the induced photoelectric properties (already alluded to above), account for the "solid-state" properties of this rigid organic solution. These two categories will be discussed in order.

A. Recombination Luminescence. Several isothermoluminescence (ITL) or "afterglow" curves are shown in Figure 3a-i for different periods of primary ionization. This luminescence consists of a mixture of fluorescence and phosphorescence of TMPD, as apparent in the data shown in Figure 3b. The kinetics of the ITL decay are complex and evidently depend on the length of the energy-storage step. When the energizing step is long enough to reach saturation, a stationary behavior is reached (see Figure 3a-i, ii) much

as is seen in photoconductivity (see Figure 2a after a total of ∼2-min irradiation). When a photosensitized sample is warmed, a very bright burst of luminescence is seen due to the collapse of the viscosity-controlled energy-storage mechanism. Recombination luminescence can also be stimulated at 77°K by using light in the visible or near-infrared region.[14,15] This is known as "stimulated emission," an effect first seen by Seebeck at the beginning of the last century in the inorganic phosphors. This terminology is not to be confused with the modern "stimulated emission" of lasers and masers. The application of an electric field also can stimulate emission[16,17] under isothermal conditions, a luminescence termed electrophotoluminescence, or (in inorganic phosphors) the Gudden–Pohl effect. Most of the studies of the recombination luminescence have centered on these two types of stimulated effects at 77°K.

In the following we are speaking of the properties of a TMPD–3MP solid at 77°K which has been *previously sensitized* by exposure to ultraviolet light in the primary region (TMPD absorption).

1. Photostimulated Emission. The Spectral and Kinetic Properties. A pulse of recombination luminescence can be excited by using infrared light (at least as low in energy at 1.6 μ) or light of higher energy up to the primary absorption region of TMPD (whereupon luminescence is directly excited once more). As in the induced photoconductivity spike, once the full course of the recombination luminescence spike is complete it can no longer be generated until the solid is sensitized anew. The spectral quality of this luminescence is demonstrated in Figure 3b, where it is seen that it represents the fluorescence and phosphorescence of TMPD but with the phosphorescence relatively enhanced by a factor of 6.6 over that under ordinary ultraviolet excitation. These spectral properties are essentially insensitive to the wavelength chosen for stimulation and furthermore are known to correspond to those of the ITL itself.

The isothermal recombination kinetics are in general very complicated. McClain[15] succeeded in deriving the observed recombination *phosphorescence* by treating the problem in which the ∼2.4-sec triplet state is driven (generated) by a recombination pulse assumed to be given faithfully by the *recombination fluorescence* signal. The fluorescing state, S_1, exhibits a 7.3-nsec lifetime[13] and is responsive to events on that time scale or longer. Stimulated recombination luminescence studies using a pulsed-laser source have shown that the actual collapse of radiatively produced mobile electrons into the trapped condition takes place in less than 1 nsec. The slow course of recombination luminescence is therefore a

(11) P. M. Johnson and A. C. Albrecht, *J. Chem. Phys.*, **44**, 1845 (1966).
(12) P. Bekowies, unpublished work in this laboratory.
(13) D. S. Kliger, J. D. Laposa, and A. C. Albrecht, *J. Chem. Phys.*, **48**, 4326 (1968).

(14) E. Dolan and A. C. Albrecht, *ibid.*, **37**, 1149 (1962); **38**, 567 (1963).
(15) W. M. McClain and A. C. Albrecht, *ibid.*, **43**, 465 (1965).
(16) G. E. Johnson, W. M. McClain, and A. C. Albrecht, *ibid.*, **43**, 2911 (1965).
(17) J. Bullot and A. C. Albrecht, *Acta Phys. Polon.*, **34**, 615 (1968). For extension of theory and experiments, see *J. Chem. Phys.*, **51**, 2220 (1969).
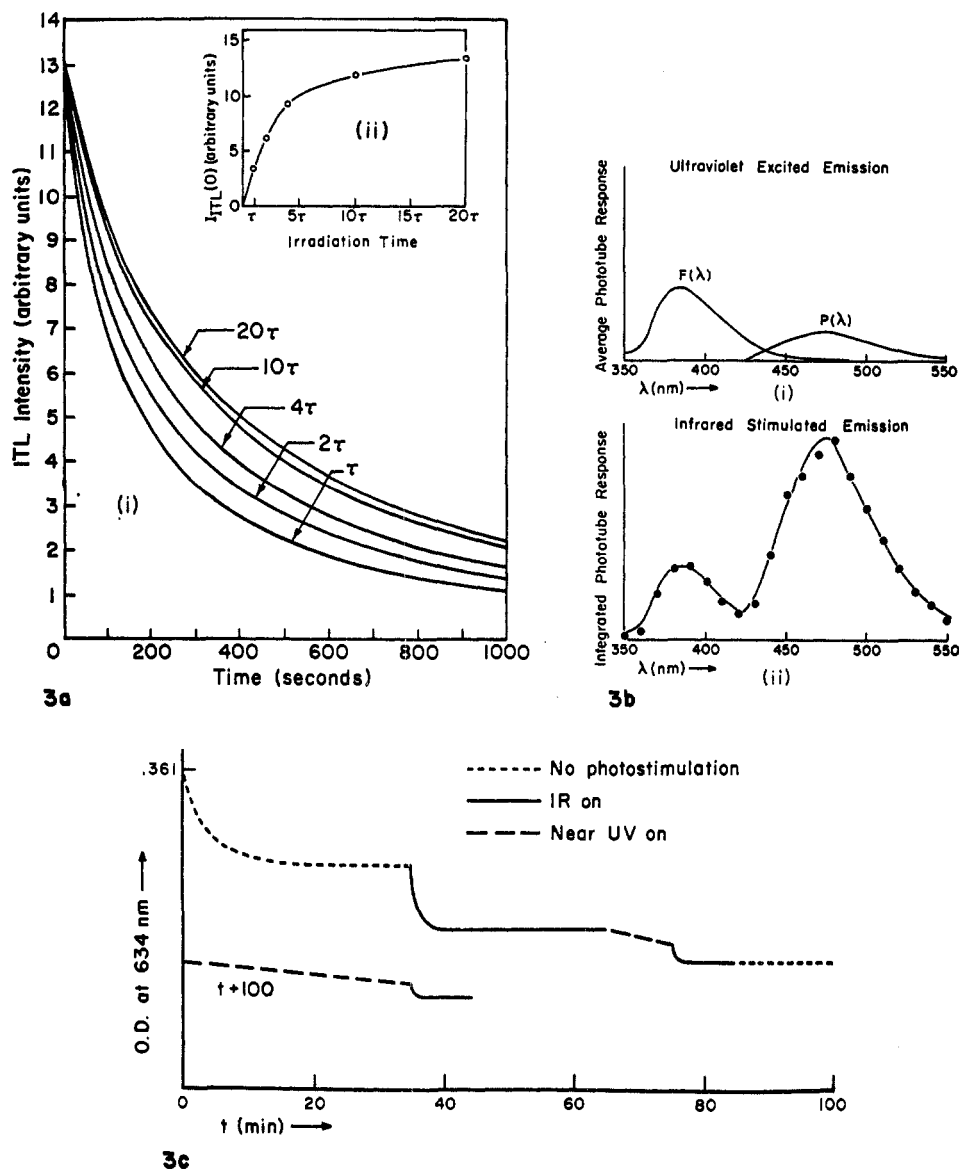
Figure 3. Recombination phenomena. (a) Isothermal recombination luminescence: (i) different ITL decays seen after varying periods of primary excitation (energy storage); each curve is scaled to $I_{ITL}(0) = 13.45$; (ii) $I_{ITL}(0)$ for increasing duration of primary excitation. The time is given in units of τ which typically is 15 sec for the monochromatic excitation employed. The initial level of ITL, $I_{ITL}(0)$, is measured following a 60-sec dark period after the primary excitation is completed. The decay curve for any one choice of primary excitation time is very reproducible while these curves vary as this time is changed. The sensitivity to irradiation time begins to vanish as the energy storage step becomes saturated ($t > 10\tau$). (See ref 17.) (b) Spectral properties of the recombination luminescence: (i) phototube response to emission of TMPD in 3-MP ($1.0 \times 10^{-3} M$) at 77°K, excited at 313 nm by an ac arc, detected by 1P21 photomultiplier through an Aminco $f/4.5$ grating monochromator; $P(\lambda)$ is the long-lived phosphorescence, while $F(\lambda)$ is the short-lived fluorescence; (ii) stimulated emission light sum spectrum. The data points were obtained by graphical integration of the stimulated emission curves when viewing at each wavelength (the sample is recycled). The large signals have proportionally larger error. The curve is obtained not from the points but from Figure 3b-i, and is given by $K[F(\lambda) + 6.6P(\lambda)]$, with K adjusted for best fit. (See ref 15.) (c) Changes in optical density (amount of WB) at 634 nm (see Figure 1) under various kinds of stimulation. The initial drop is due to "thermal stimulation" at 77°K ($kT \cong 6 \times 10^{-3}$ eV). The infrared photons used are about 0.8 eV and the near-ultraviolet photons are 3.2 eV. When the ir is on, the uv is off, and vice versa. $- - -$, no photostimulation; $\qquad$, ir on; $- - - -$ near-uv on. (See ref 15.)

measure of the slow rate of *producing* mobile electrons and does not reflect the rate of diffusion of the electron in the mobile condition. Indeed, in stimulated emission, as the stimulating light is focused, the recombination fluorescence spike becomes increasingly sharp and its decay becomes more and more exponential. Furthermore, the decay constant is now linear in the intensity of the stimulating beam. A lifetime as short as 30 msec has been obtained.[18]

2. The Bleaching of Wurster's Blue. Another measure of the recombination process is the bleaching of the blue coloration of WB. By monitoring the optical density at 634 nm, McClain was able to display recombination events achieved under successively more energetic conditions of stimulation (Figure 3c). The initial bleaching effect is due to isothermal recombination.

(18) D. Myers, unpublished work in this laboratory.

This is followed by infrared stimulation. The combined effect in this example is to bleach approximately one-half of the cation (and this could have been accomplished entirely by photostimulation had that been carried out at $t = 0$). A more quantitative examination of the expected link between bleaching and recombination luminescence shows that the amount of bleached WB at any time, t, is found to be proportional to the total recombination luminescence light sum up to that time.[15] The recombination of electrons with a partially oriented WB population gives a *polarized* recombination luminescence, and this has been used in an interesting fashion by McClain[19] to explore the question of correlated *vs.* uncorrelated ionizations. The overall picture derived largely from electrophotoluminescence studies,[17] extension of the polarized recombination luminescence work,[18,19] and kinetic studies at high levels of infrared stimulation[18] is as follows. At low conversions, the majority of electrons remain correlated with their center of origin and in fact are probably located between ~10 and 40 Å from the cation.[17] After prolonged exposure to ionizing light, a steady-state situation is reached in which a significant fraction of the electrons have escaped the Coulomb well of the cationic center of origin, giving rise to uncorrelated charge pairs.

3. Electrophotoluminescence. The photoconductivity work naturally provided an environment in which a high electric field could be applied to the sensitized solid. When this was done in the presence of a photomultiplier, a sharp enhancement of the ITL was observed.[16] The early observations of this electrophotoluminescence (EPL) in TMPD–3-MP solid have been greatly extended by Bullot.[17] The EPL signals in the TMPD–3-MP solid at 77°K are clearly seen at applied fields of ~2 × 10⁵ V/cm and upward, and the field (E) dependence of the EPL spike height is exactly exponential. If we assume that this is a Boltzmann factor, then the exponent will be dE/kT. With $kT = 0.006$ V at 77°K, the coupling parameter, d, can be determined. Over a number of experiments it is found to lie in the range from 0.9 to 1.9 Å, and the value found for any one sample is quite reproducible.

It was further discovered that once an EPL spike has run its course with the dc field applied in a given direction it was possible, *without* resensitizing the solid, to generate another EPL spike very similar to the first one *when the applied field is reversed.* Once both spikes have been emitted, then new EPL signals are seen only following renewed sensitization. Data related to EPL studies are depicted in Figure 4. The two-spike EPL property is clearly illustrated in Figure 4a. This two-spike behavior has been fundamental in the development of a model for the solid-state behavior of this system. Upon further study, it is found that this two-spike behavior loses its symmetry as soon as the primary ionization step approaches steady-state conditions.

This loss of symmetry is understood as a sign of a significant presence of uncorrelated charges.

After developing a model to explain this EPL behavior, it became clear that the model contained a prediction of *negative* EPL. That is, after a very long imposition of the applied field its *removal* should bring about an *increase* in recombination luminescence. Such signals are indeed seen and are illustrated in Figure 4b following nearly 15 min of a field-on condition.

B. Photoconductivity in the Sensitized Solid. The photoconductivity spike seen in the previously sensitized solid is intimately tied to that of the stimulated emission spike. In Figure 5[20] the two signals are shown simultaneously detected in one sample with varying dark intervals separating the energy-storage step from the light-stimulating step. These signals are closely tied to the trapped electron. The quasistationary signal seen when exciting just to the red (say at 365 nm) of the primary absorption region must be different in origin. Unlike the spike signal, this signal is not sensitive to the softening of the matrix or to the adding of scavengers. Neither the 365-nm type of induced signal nor, of course, the spike-type signal is unique to the TMPD–3MP system. When methylated benzenes replace TMPD as the solute, qualitatively similar patterns are seen.[6]

It was found[6,7] that the spiking builds up with the square of the primary light intensity as expected. Furthermore, the spike height itself is linear in the stimulating intensity. Thus, the matrix-trapped electron is produced by *two photons* and ionized by *one photon*. In contrast to this, the initial buildup of 365-nm sensitivity (the quasistationary signal) was found to be more nearly *linear* in the primary light level. The state responsible for this signal (which is one photon produced) appears to be one photon ionized,[6] although a biphotonic component may also be present.[7] The spike signals are readily understood as representing the rapid bleaching of biphotonically produced matrix trapped electrons as they are photomobilized (one photon) and then rapidly fall into Coulomb capture by the cationic centers. However, elucidation of the origin of the "365" induced signal will require much more detailed study.

A Model for the Photosensitized Solid and Rationalization of Its Properties

The main features of the model for the sensitized rigid organic solution actually have appeared throughout the material already presented. Its central features are the following. (1) Electrons are the major charge carrier. (2) The rigid solution contains electron-trapping sites (thought to be preexisting matrix cavities) homogeneously dispersed throughout the solid. At a concentration of $>10^{-2}$ M these trapping sites are on the average no more than ~50 Å apart. At 77°K

(19) W. M. McClain and A. C. Albrecht, *J. Chem. Phys.*, 44, 1594 (1966).

(20) A. C. Albrecht, P. M. Johnson, and W. M. McClain, Proceedings of the International Conference on Luminescence, Budapest, 1966, p 405.

4a — EPL Decay with reversal of the field. Field strength 0.4×10^6 Vcm^{-1}. — experiment, ••• theory. Luminescence Intensity (arbitrary units) vs Time (seconds). +2000V on, off, −2000V on, τ_1, τ_2.

4b — EPL (—), ITL (- - -). I_{EPL} (arbitrary units) vs Time (sec.). τ_1 OFF, τ_2 ON, τ_3 OFF, τ_4 ON, τ_5 OFF, ×15.

4c — $\frac{a}{2} I_{ITL}(at)$ or $a^{-1}\frac{a}{2}I_{ITL}(a^{-1}t)$ vs Time (sec). — 0.8×10^6 Vcm^{-1}, - - - 0.4×10^6 Vcm^{-1}. Group I, Group II.

4d — $\mathcal{I}_{EPL}$ (arbitrary units) vs $a^2 I_{ITL}(at+\theta)+I_{ITL}(a^{-1}t+\theta')$.
$\tau_1 = \tau_2 = 30$ seconds, $a = 3.0$.
○ first field application $\theta = \theta' = 0$
● second field application in opposite direction
$\theta = \tau_1(a^{-1}-a)+\tau_2(1-a)$
$\theta' = \tau_1(a-a^{-1})+\tau_2(1-a^{-1})$
△ second field application in the same direction
$\theta = \tau_2(1-a)$
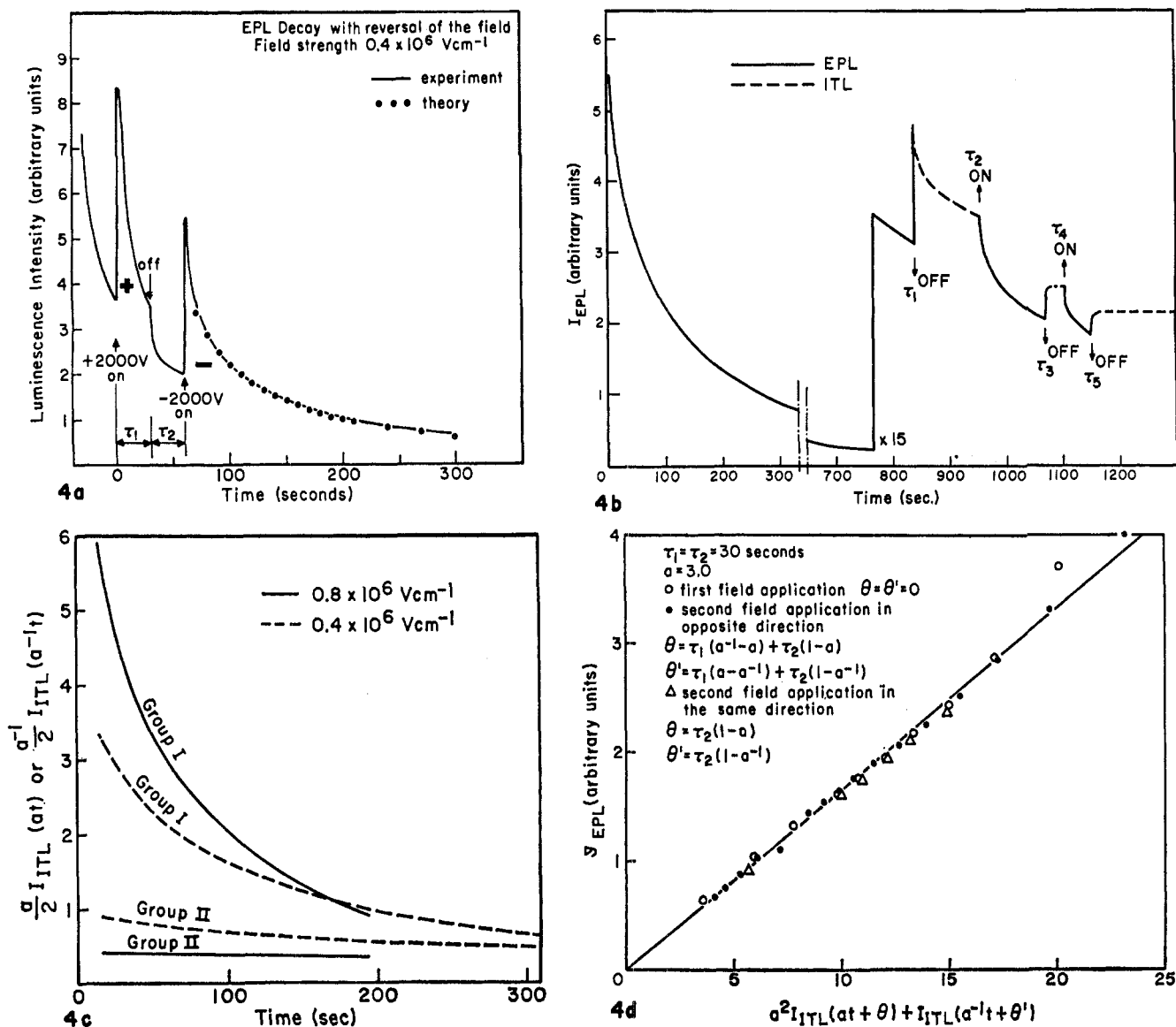$\theta' = \tau_2(1-a^{-1})$

Figure 4. Electrophotoluminescence data. (a) Typical EPL signals seen in a photosensitized solid at 77°K. The ITL signal seen at the start of the plot is measured following a 60-sec dark period subsequent to uv sensitization (its level is typically $\sim^1/_{50}$ of the normal uv-excited emission). At $t = 0$ an electric field is applied to the sample and the EPL spike is seen for $\tau_1 = 30$ sec. At $\tau_2 = 30$ sec a field-off period ensues during which time a new ITL decay is achieved. Then the field is applied in the opposite direction to give an EPL spike very much like the first. Subsequent applications of field lead to little or no further EPL unless the sample is sensitized anew. The dotted curve represents the fit to experiment obtained from theory (see text). (See ref 17.) (b) An example of *inverse* EPL. This figure shows an EPL signal which has been extended to 825 sec. At that point, τ_1, the field is removed and an ITL decay is seen which is greater than the previous EPL level. Normally (see Figure 4a) the ITL level is below the EPL signal. Reapplication of the field at τ_2 quenches the luminescence. An additional inverse EPL signal is seen at τ_3. The transition from ordinary EPL to this inverse EPL behavior occurs only following lengthy application of the field. (See ref 17.) (c) A plot of the time decay of group I (accelerated) electrons and of group II (retarded) electrons at two different field strengths (from eq 1). The two groups of electrons are not mutually thermally equilibrated on this time scale. (See ref 17.) (d) A test of eq 2 for three different experiments. Prediction of time course of EPL upon: ○—○, first applying a field to a photosensitized sample (first spike in Figure 4a); ●—●, then applying a field in the opposite direction after a 30-sec field-off period (see fit by theory shown in Figure 4a); △—△, applying a field in the second application with the *same* sign as in the first after a 30-sec field-off period (the second spike is now much weaker than that shown in Figure 4a). The fit shown here for a single parameter, $a = 3.0$, is equivalent to an actual agreement between theory and experiment, in each case, as good as the fit illustrated in Figure 4a for the ●—● case. (See ref 17.)

and in 3-MP the matrix-trapped electron may live as long as several minutes. Electrons in the trapped state are assumed to be immobile (no tunnelling). (3) A *mobile* electron is one which has escaped from a trapping site (or has just been produced through solute ionization). We take it to be locally thermalized and consider it to be mobile as long as it moves among "energy ripples" which are no more than kT deep.

These "ripples" are necessarily present because of the discrete molecular and atomic structure of the solvent. In one limit, these energy "ripples" can originate from the uncertainty principle. Whatever these details, the half-life of the mobile electron is less than 1 nsec.[13] It follows that under no conditions employed in our work is the number density of mobile electrons, n, significant from the point of view of material balance; that
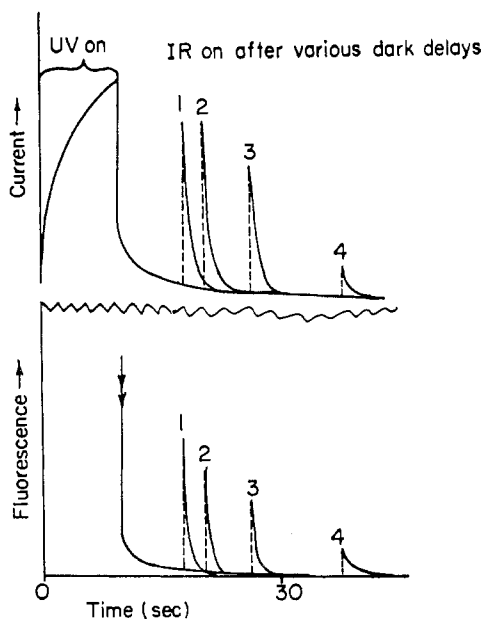
Figure 5. A simultaneous study of induced photoconductivity spikes and infrared recombination luminescence spikes in the same sample. The induced signals are stimulated after varying dark periods following the uv-sensitization step. The sample must be resensitized after each application of infrared light. The gross similarity of the two signals speaks for their common origin (the matrix-trapped electron). The successive weakening from peaks one to four is indicative of the increased thermal recombination of trapped electrons with successively longer dark periods. Since photoconductivity measures Coulomb *liberated* charges while recombination luminescence measures Columb *capture*, the detailed time behavior of any one spike is different for each type of signal (this is not evident here). (See ref 20.)

Figure 6. The Coulomb well, due to the WB cation, drawn for a medium having a dielectric constant of ~ 2. The notation is self-explanatory and was developed for treating the kinetics of photoionization. Certain properties of trapped electrons A_2' and A_3' differ because of the changing Coulomb force as a function of position. The energy curve reaches about 6 eV above S_0 (ground-state TMPD) at infinite charge separation for the TMPD–3MP system. (See ref 7.)

is, $n \lll N$ (where N is the number density of trapped electrons). (4) The rigid solution, after primary ionization, is inevitably permeated by long-range Coulomb fields centered on the cation (as an attractive potential) and centered on the trapped electron (as a repulsive potential). The mobile electron moves in a superposition of these potentials added to the short-range effects due to the neutral trapping cavities. An externally applied field can considerably perturb this picture.

That the Coulomb potentials must be long range follows from the low dielectric constant of the medium ($\epsilon \cong 2$). The superposition of the neighboring cation potentials brings the average Coulomb escape distance to a value of the order of 500 Å. An important fact is that the region within which the electron is bound to its cationic center (from which a mobilized electron cannot thermally escape) contains about 10^3 electron-trapping sites. The preexisting sites are presumably homogeneously distributed throughout the medium with little or no specific correlation to the neutral solute molecules. Thus, as a cationic Coulomb center suddenly appears, a great many of the sites find themselves in the Coulomb gradient well *within* the escape distance for a mobile electron. One branch of such a Coulomb well showing two trapping sites, A_2 and A_3, is illustrated in Figure 6.

The Coulomb gradient becomes very strong near the cation, and this must have a profound effect on the
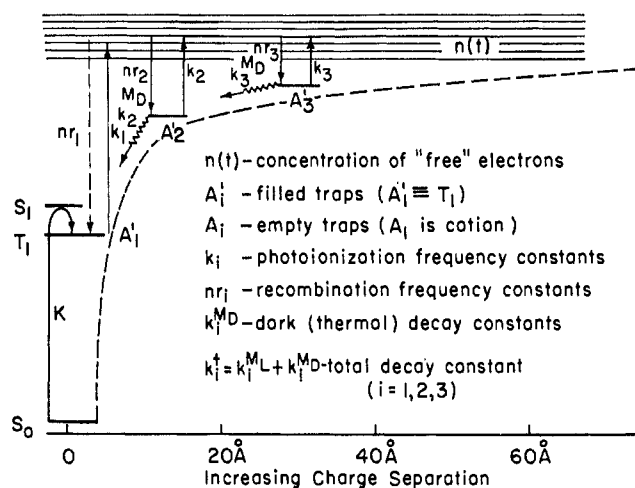
lifetime of the electron trapped in a cavity very near a positive center. In fact the EPL work has demonstrated the coupling of the trapped electron with an (external) electric field, and a value for the coupling parameter has been obtained. An activation process (Boltzmann factor) is implicated. The internal Coulomb field can be estimated ($e^2/(\epsilon R^2)$) and be introduced as a perturbation into the exponential form of the activation process. The rate constant for thermally mobilizing the ith trapped electron, k_i^{MD}, can now be written as a function of position, R, in the Coulomb gradient of the cation. Thus $k^{\mathrm{MD}}(R) = k^{\mathrm{MD}}(\infty) \exp [(e^2 d/\epsilon R^2)(kT)^{-1}]$ where d is the coupling parameter (0.9 to 1.9 Å) obtained in the EPL work. Now k^{MD} is just the reciprocal dark lifetime, τ_D^{-1}, of a trapped electron, and it is seen how it is extremely sensitive to the position, R, of the electron in the Coulomb well. An electron at 10 Å has a lifetime about 2000 times shorter than the value at $R = \infty$ (or, practically speaking, $R \gtrsim 50$ Å). It is now believed that this simple, but dramatic, distribution of lifetimes must be responsible for the complicated isothermal recombination kinetics. The fact that electrons trapped very near the Coulomb center are subject to very high electric fields, and therefore are very short lived, forbids their participation in the energy-storage step. Only those electrons which are trapped for minutes or longer qualify, and in 3-MP these must be located at least tens of ångströms from the cationic center. A glance at Figure 6 shows that the energy requirement for producing such electrons approaches that for complete ionization (not much below the gaseous ionization potential in the low dielectric constant medium). *The biphotonic* requirement for storage of energy, much less for Coulomb escape (photoconductivity), now becomes self-evident.

It is not difficult to argue that the rate constant for

photomobilizing the *i*th trapped electron, $k_i{}^{\text{ML}}$, is *not* dependent on R since this is related almost entirely to the *local* trap depth at any R. The single, broad, near-infrared cross section for mobilizing trapped electrons[21] speaks for this. Also the ability[18] to convert the complex decay kinetics to a simple exponential decay under sufficiently intense infrared stimulus is thus explained (*i.e.*, $k_i{}^{\text{ML}} \gg k_i{}^{\text{MD}}(R)$ where $k_i{}^{\text{ML}}$ is the same light-governed constant *for all electrons at any position* in the Coulomb well). On the other hand the cross section for photoionization (full charge separation) with photoionization constant, k_i, for the *i*th trap possesses a threshold which must blue shift in proportion to $1/R$. The threshold for ionization (Coulomb escape) of A'_2 in Figure 6 is clearly greater than that for A'_3. Threshold studies for photoconductivity signals (photoionizations) on the one hand, and stimulated recombination luminescence (photomobilization) on the other, have simply not been carried out to test these predictions. We do not yet even know the fraction of charge pairs which leads to photoconductivity. Nevertheless, these general ideas have played an important role in understanding the rise kinetics of the photocurrents especially under broad-band or double-beam excitation.[7]

This model has been extremely fruitful in understanding the EPL results. When it is assumed that the trapped electrons, as well as mobile electrons, are subjected to some uniform perturbation and ordinary diffusion theory is examined, it is found that the new, perturbed recombination kinetics can be simply related to the unperturbed kinetics by *scaling the time and the amplitude by a common factor*, a, which is exponential in the perturbation. (It is assumed that the diffusion of the mobile electron itself is an activation process—as is certainly the case for mobilizing the trapped electron.) A temperature jump would be an excellent example of such a uniform perturbation. When the perturbation is an externally applied, homogeneous electric field its unidirectional nature forces one to distinguish *two groups of electrons* by virtue of their positions in the internal Coulomb fields of the cationic centers. As long as the recombination step is controlled by these fields, one-half of the electrons (called group I) approaches their Coulomb center *with* the applied field, the other half (group II) *against* the applied field. The applied field *accelerates* the recombination of group I while it *retards* the recombination of group II. A glance at Figure 7 clarifies this. If one clings to this simple "one-dimensional" approach one obtains the following simple equation (eq 1) relating the observed time course of the EPL signal to the ITL kinetics in the same sample by a single scaling parameter.

$$I_{\text{EPL}}(t) = \frac{a}{2} I_{\text{ITL}}(at) + \frac{a^{-1}}{2} I_{\text{ITL}}(a^{-1}t) \qquad (1)$$

$$\underbrace{\hphantom{\frac{a}{2} I_{\text{ITL}}(at)}}_{\text{group I}} \qquad \underbrace{\hphantom{\frac{a^{-1}}{2} I_{\text{ITL}}(a^{-1}t)}}_{\text{group II}}$$

(21) See, for example, J. B. Gallivan and W. H. Hamill, *J. Chem. Phys.*, 44, 1279 (1966); see also J. Bourguignon, Senior Honors Thesis, Cornell University, June 1963.

a. Field Off: ITL   b. Field On: EPL (+)

c. After Long EPL(+): Low Light Level

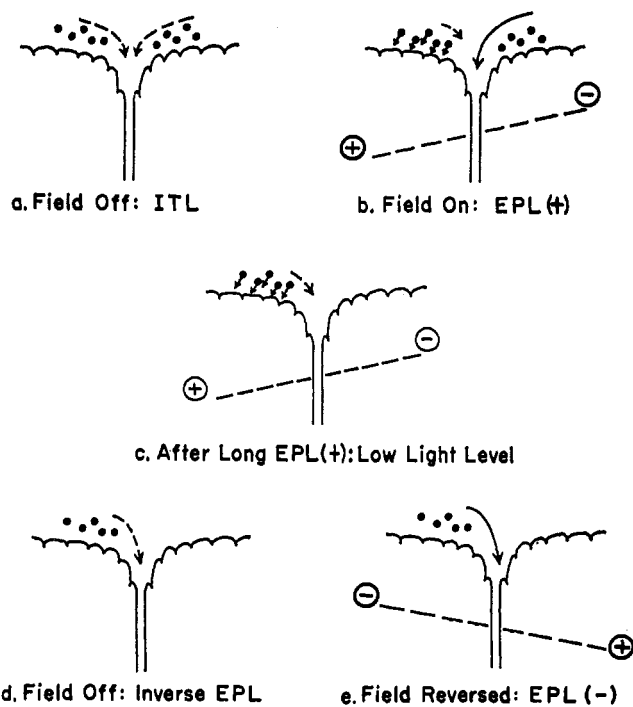d. Field Off: Inverse EPL   e. Field Reversed: EPL (−)

Figure 7. Qualitative aspects of the Coulomb well model in which the recombination is Coulomb-field governed. (a) Normal inward flow giving ITL. (b) An EPL signal due to acceleration of the right (group I) electrons. (c) After long EPL signal group I electrons are depleted. The signal is now like that in Figure 4b just prior to removal of the field. (d) Removal of the field releases the previously retarded group II electrons exhibiting an inverse effect in which removal of the field *raises* the light level (see Figure 4b). (e) Reapplication of the field in the reverse direction at any stage gives a new, strong EPL spike, as group II electrons previously retarded are now accelerated. The gradient of the applied field shown here is exaggerated. In fact, where electrons are found, it must not exceed the Coulomb gradient (within the approximation of the model employed).

Here $a \geq 1$ and, because it is exponential in the perturbation, it appears reciprocally in the acceleration of group I and the retardation of group II electrons. This equation has met with surprising success, and the exponential dependence of a on E has been confirmed to give the coupling parameter, d, already referred to. Just one example of the success of eq 1 is the fit exhibited in Figure 4a of the negative-field EPL decay seen following τ_1 sec of positive-field EPL and τ_2 sec of field-off ITL decay. The independent behavior of groups I and II electrons at two different field strengths is illustrated in Figure 4c. The acceleration of group I and retardation of group II are clearly apparent.

Equation 1 has been easily generalized to treat a variety of histories of field-on field-off decays. Thus

$$I_{\text{EPL}}(t) = \frac{a}{2} I_{\text{ITL}}(at + \Theta) + \frac{a^{-1}}{2} I_{\text{ITL}}(a^{-1}t + \Theta') \qquad (2)$$

where Θ and Θ' are defined for different cases as

Θ	Θ'	$I_{\text{EPL}}(t)$
0	0	$I_{\text{EPL}}(t)$
$\tau_2(1 - a)$	$\tau_2(1 - a^{-1})$	$I_{\text{EPL}}{}^2{}^+(t)$
$\tau_1(a^{-1} - a) + \tau_2(1 - a)$	$\tau_1(a - a^{-1}) + \tau_2(1 - a^{-1})$	$I_{\text{EPL}}{}^\pm(t)$

Here τ_1 is the duration of the first EPL period and τ_2 is the duration of the field-free period prior to the second

application of the field which is in the same direction for $I_{\text{EPL}}^{2+}(t)$, or in the opposite direction for $I_{\text{EPL}}^{-}(t)$. A factor $(a^{-1}/2)$ may be removed from eq 2 to suggest the plot presented in Figure 4d where eq 2 is successfully tested for all three types of signals with one value for the parameter a. Figure 4a shows the actual fit for the $I_{\text{EPL}}^{\pm}(t)$ signal.

A summary of the Coulomb well model with its expected EPL properties is qualitatively offered in Figure 7. The quantitative success of eq 1 (and eq 2 which is derived from it) appears to be the single most clearcut demonstration that the vast majority of ionized electrons are Coulomb bound to cationic centers—at least until the energy-storage step approaches saturation of the system and eq 1 fails. The intimate connection between ITL and EPL through eq 1 implies that *all* electrons active in the ITL process are also involved in the EPL behavior.

The requirement (in the theoretical basis of eq 1 and 2) that the recombination be governed by the Coulomb field and only perturbed by the external field places an upper limit of $R = 30\text{--}40\,\text{Å}$ on the location of the trapped electrons in the Coulomb well. At these distances the applied field and the Coulomb field are similar in magnitude.[22] At the same time the very short life of cavity traps at $R \gtrsim 10\,\text{Å}$ (even with an $R = \infty$ lifetime of hours) places a lower limit on the acceptable values of R as we have seen. The consequences of the model, therefore, call for a fairly narrow range of electron distribution ($10\,\text{Å} \gtrsim R \gtrsim 40\,\text{Å}$) about the cationic center at the initial stages of ionization. Especially astonishing is the complete success of a simple *one-dimensional* model. In an expected three-dimensional distribution of electrons about Coulomb centers, one must consider the inwardly directed components of the unidirectional applied field which vary smoothly from a minimum through zero to a maximum. That is, the parameter, a, must be a function of position. Equation 1 is lost when attempts are made to introduce this refinement. The call for one-dimensionality must be either an artifact of the model, where an entirely different model (three dimensional) might lead to an equation like eq 1, or this one-dimensionality carries real physical significance. We are inclined toward the latter view. It must be pointed out first that in EPL, ITL, and photoconductivity studies the organic solid is more nearly a two-dimensional thin film with all that that implies, and, secondly, the primary process in photoionization does not cause electrons to be ejected with

equal probability in all directions. Furthermore, the independent behavior of groups I and II electrons as illustrated in Figure 4c and implicit in the success of eq 1 indicates that these electrons are *not* capable of mutual thermal equilibration on the time scale of many minutes.

Conclusion

Evidently as long as one maintains a proper balance between energy-storage ability (the fixing of ionization) and the energy release (the release of ionization) one will have a phosphor-like organic solid. If one were willing to compress the time scale to microseconds or nanoseconds and use very intense flashes (lasers) in the energy-storage steps, then perhaps most fluid organic solutions should exhibit similar behavior. In any case, as long as low dielectric constant media are used the Coulomb forces will play a dominant role both in the energy-storage step (where a two-photon requirement will be likely) and in the mechanism of delayed energy release. Furthermore, as a rigid solid is softened the mobilization of the trapped electron will very likely be increasingly governed by *structural* relaxations of the solvent which we suspect (but are not certain) are not playing a dominant role in 3-MP at 77°K.

Whether these organic solids with their phosphor-like properties shall prove to be of "practical" value is a question for the future. An important step in this direction would be to design room-temperature versions of these solids, a problem which may be difficult in principle if cavity trapping is still to be the principal mode of fixing the energy storage. At room temperature kT may now easily overcome the "natural" barrier heights to be associated with cavity trapping. What is already clear is that these systems are very inviting for fundamental studies in the mechanisms of photoionization, electron trapping, electron mobility, and electron-cation recombination phenomena in organic materials. Finally, it seems reasonable to expect that studies of this kind will ultimately be able to contribute to our understanding of the structure of organic liquids.

(22) The effect of an applied field on grossly distorting a Coulomb potential in a solid seems to have been discussed first by J. Frenkel, *Phys. Rev.*, **54**, 647 (1938). Whereas Poole's law leads to an exponential in E deviation from Ohm's law (as seen in our solids), the Frenkel effect is exponential in $E^{1/2}$. Recent work on amorphous selenium films appears to demonstrate the $E^{1/2}$ Frenkel effect on carrier generation: D. M. Pai and S. W. Ing, Jr., *Phys. Rev.*, **173**, 729 (1968); M. D. Tabak and P. J. Warter, Jr., *ibid.*, **173**, 899 (1968).